



Peyton, Anthony, Karimian, Noushin, Wilson, John, Stolzenberg, M, Schmidt, R, Davis, Claire, Lombard, P, Meilland, P, Martinez-de-Guerenu, A and Gur-ruchaga, K (2016) The application of electromagnetic measurements for the assessment of skin passed steel samples. In: 19th World Conference on Non-Destructive Testing (WCNDT 2016), 13 June 2016 - 17 June 2016, Munich, Germany.

Downloaded from: <https://e-space.mmu.ac.uk/626756/>

Version: Published Version

Usage rights: Creative Commons: Attribution 4.0

Please cite the published version

<https://e-space.mmu.ac.uk>



The Application of Electromagnetic Measurements for the Assessment of Skin Passed Steel Samples

Anthony PEYTON¹, Noushin KARIMIAN¹, John WILSON¹, Mathias STOLZENBERG²,
René SCHMIDT³, Claire DAVIS⁴, Lei ZHOU⁴, Patrick LOMBARD⁵,
Philip MEILLAND⁶, Ane MARTINEZ-DE-GUERENU⁷, Kizkitza GURRUCHAGA⁷

¹ University of Manchester, Manchester, UK

² Salzgitter Mannesmann Forschung GmbH, 38239 Salzgitter, Germany

³ ArcelorMittal Eisenhüttenstadt GmbH, Germany

⁴ University of Warwick Warwick Manufacturing Group (WMG), Coventry, UK

⁵ CEDRAT, Meylan, France

⁶ Arcelor Mittal Global Research and Development Maizières Process, Maizières-lès-Metz
Cedex, France

⁷ CEIT, San Sebastián, Spain

Contact e-mail: a.peyton@manchester.ac.uk

Abstract. This paper begins by exploring the relationship between magnetic properties such as coercive field, RMS Magnetic Barkhausen Noise (MBN), initial and differential permeability and percentage elongation of skin passed samples for three different steels; interstitial free, micro alloyed and dual phase. A closed magnetic loop system is used to measure the fundamental magnetisation properties and a system based on an impedance analyser and a cylindrical coil is used to determine low field differential permeability. The results show that coercive field increases consistently with increasing percentage elongation for all three steels, as increasing material hardness causes an increase in magnetic hardness and a corresponding increase in coercive field. This effect levels off at higher values as dislocation density saturates. As would be expected, the inverse trend is observed for differential permeability. Similar results are also reported for MBN and initial and low field differential permeability measurements for the interstitial free and dual phase steel, but the behaviour for the micro alloyed samples appears to be more complex.

Finally, the paper considers the response of two on-line measurement systems that exploit these magnetic relations. The first system applies pulse excitation and measures the resulting remnant magnetisation and the second analyses the harmonic response from AC excitation. Both systems can detect microstructural changes associated with varying magnetic properties during strip production.

1. Introduction

Skin pass rolling is used after cold rolling and annealing of steel strip to ensure a consistent yield point for the material, set the desired surface roughness and control strip thickness and flatness. Both the magnetic and mechanical properties of steel strip are affected by skin pass rolling through, for instance, the influence of the dislocation density generated. Therefore, in order to optimise the final properties it is desirable to control the skin pass



rolling process through in-situ monitoring of material properties by exploiting magnetic and electromagnetic measurements.

This paper explores the link between the magnetic properties such as coercive field, RMS Magnetic Barkhausen Noise (MBN), differential, initial and low field differential permeability and percentage elongation of skin passed samples for three different steels; interstitial free, micro alloyed and dual phase. Following this the paper considers how these relationships can be exploited and presents results from two on-line systems.

2. Magnetic Measurements

In this section, several types of magnetic measurements are presented. All measurements were made using test systems developed at CEIT, Spain and at the University of Manchester, UK. Further details of the test systems and procedures can be found here [1-3].

2.1. Sample preparation

Skin passed samples were prepared at the SZMF laboratory from IF-260 interstitial free (IF), 340-LAD micro-alloyed (MA) and DP-600 dual phase (DP) galvanized steels. Original samples prior to on-line skin passing could not be extracted; therefore there is no baseline (or “null”) skin pass deformation measurement for these samples. Samples were obtained with 0.9%, 1.2% and 0.2% initial equivalent elongation levels for the IF, MA and DP steels, respectively, with the laboratory skin pass elongation values used being cumulative to this. Smaller sections were machined from the laboratory skin pass samples for magnetic testing. The magnetic test samples are 5 mm in width, with lengths ranging from 130 mm to 150 mm and final thicknesses ranging from 0.877 mm to 1.005 mm.

Fig. 1 shows a plot of the thickness of the samples against final deformation levels after adding the deformation level from finishing and the laboratory skin pass deformation (percentage elongation). Test results in the remainder of this paper are plotted against this measure of total percentage elongation. It can be seen from Fig. 1 that the DP samples show the greatest change in both elongation and thickness, with a large reduction in thickness for the first 2% elongation. There is a more linear relationship between thickness and elongation for the IF samples and a very small change in both for the MA samples.

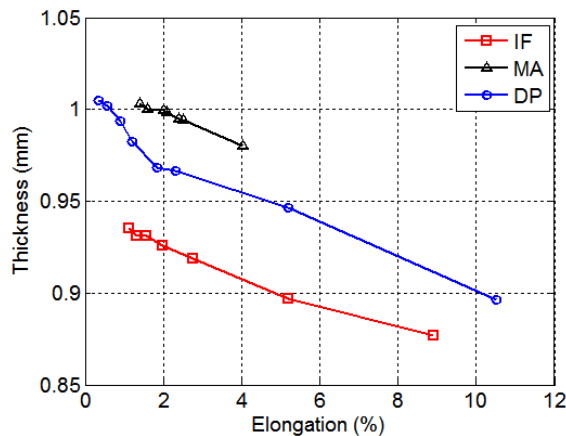


Fig. 1. Thickness for total percentage elongation for all sample sets

2.2. Major BH loop and differential permeability

Fig. 2 shows major BH loops and differential permeability curves for all three sample sets. The change in the shape of the loop is similar for all materials; elongation of the loop, coupled with widening of the loop around the B=0 point (coercive field). This change in the shape of the loop is typical of material under compressive stress or material hardening.

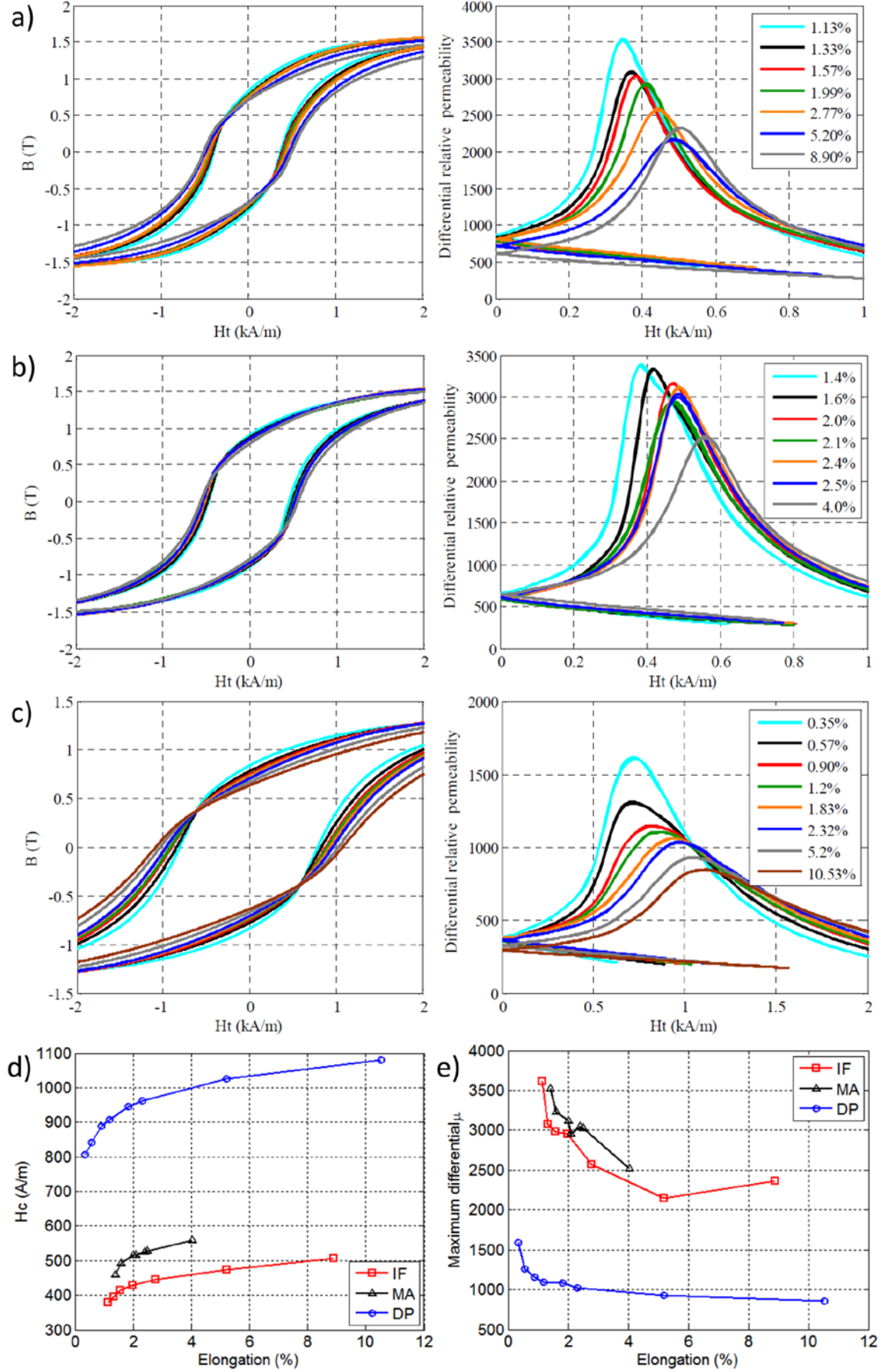


Fig. 2. BH loops and differential permeability curves for IF (a), MA (b) and DP (c) sample sets. Changes in coercive field (d) and maximum differential relative permeability (e) for increasing elongation

Fig. 2d shows the coercive field values derived from the major loops. It can be seen from the plot that there is a large initial increase in coercive field, consistent with an increase in magnetic hardness, which in turn is indicative of an increase in mechanical hardness. After around 2% elongation, the curves level out, indicating a saturation of dislocation density. The maximum differential permeability curves (Fig. 2e) show a reciprocal decrease with increasing percentage elongation consistent with increasing magnetic hardness.

2.3. Magnetic Barkhausen Noise

Fig. 3a shows a plot of the RMS MBN measurements. The DP sample exhibits an initial small increase followed by larger decrease. For the IF sample, the peak in the RMS MBN comes at a higher level of percentage elongation. The values level off for both sample sets at higher levels of elongation, indicating a saturation of dislocation density in the material. The MA sample set shows a characteristic ‘M’ shape, shared by the initial permeability results shown later in this paper. The plots of the MBN peak position (Fig. 3b) exhibit an increase similar to that shown by the coercive field in Fig. 2d. This shift in maximum MBN activity to a higher applied field is consistent with an increase in magnetic hardness.

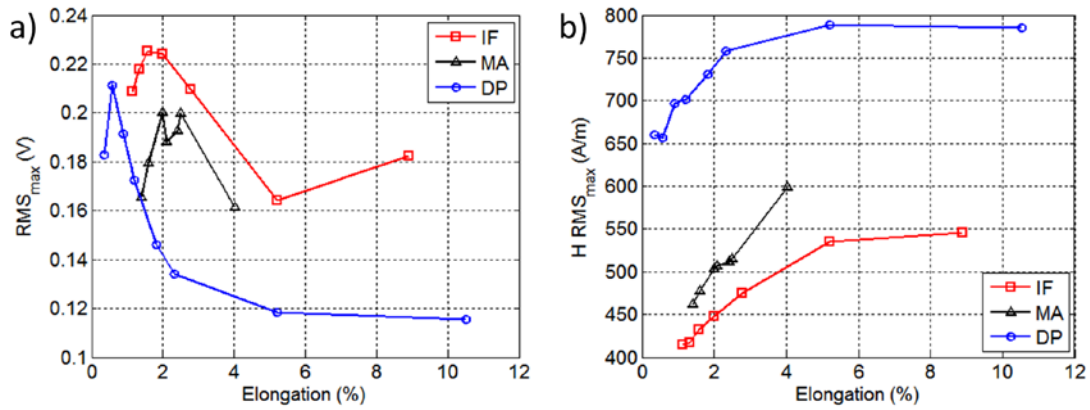


Fig. 3. MBN measurements: a) Amplitude of the peak of the MBN envelope or RMS profile of MBN; b) Position of the peak of the MBN envelope in terms of intensity of the tangential magnetic field

2.4. Initial and low field differential permeability

The plot shown in Fig. 4a is initial permeability derived from direct measurements of B and H, using an excitation core with an encircling coil to measure B and a Hall sensor to measure H [3], with values calculated from the relationship $\mu_i = \Delta B / \Delta H \cdot \mu_0$. Fig. 4b is derived from mutual inductance measurements using a solenoid sensor and impedance analyser, where the low field differential permeability values were calculated by fitting the experimental data to finite element models [1].

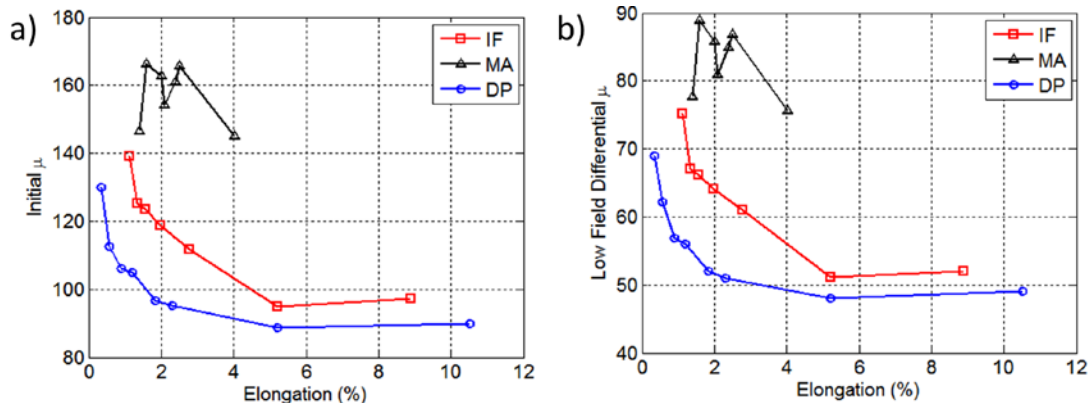


Fig. 4. a) Initial permeability derived from direct measurement of minor loops using U-core measurement system ($\mu_i = \Delta B / \Delta H \cdot \mu_0$), b) Low field differential permeability derived from solenoid sensor

Comparison of the plots from the two systems shows that the values follow the same general trend for all sample sets; for IF and DP, a sharp decrease followed by a levelling out as dislocation density saturates, for MA, a non-monotonic ‘M’ shaped signal. The higher amplitude of the initial as compared to the low field differential permeability is due to the higher loop amplitudes used for the initial permeability measurements. At higher applied field values, more energy is applied to domain walls, so more pinning sites can be overcome, leading to a greater ΔB for a given ΔH .

3. Measurements from Harmonic Analysis Coil Online Measuring (HACOM) system

3.1. HACOM test system

The HACOM system was developed at the Institute for Material Science (IW) of the University of Hannover, Department of Nondestructive Testing (ZfP) and is employed at Salzgitter Flachstahl GmbH (SZFG) in the continuous operation of a hot-dip galvanizing line. It provides non-destructive determination of direction-dependent mechanical material properties such as yield strength (R_m) and tensile strength ($R_{p0.2}$) as well as material properties such as anisotropy and strain hardening. Sinusoidal magnetisation of the sample at a low flux density far from saturation is employed at four frequencies between 20 Hz and 5 kHz. The magnetisation of the sample will run through hysteresis loops, exciting induction signals in a receiving coil. An FFT is performed to gain the harmonic spectrum. Due to symmetry reasons only odd harmonics will appear in the sine and cosine terms. These are evaluated up to the 5th harmonic for 4 different frequencies. So a set of 4x12 amplitude values for regression analysis is used. This method is described in detail in [4]. The laboratory based HACOM system used for the measurements is shown in Fig. 5.

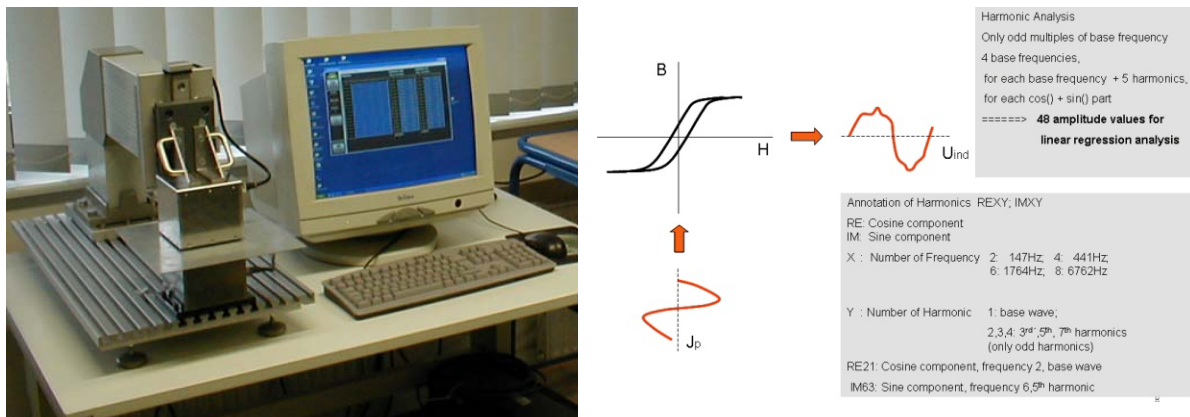


Fig. 5. a) Laboratory HACOM test system, b) Harmonic analysis of measured signal

3.2. HACOM laboratory measurements

Fig. 6 shows a plot of the real and imaginary signal components from the lab-based HACOM system. It can be seen from the plots that for IF and DP steels the HACOM signal decreases monotonically with increasing percentage elongation. For the MA steel, the plot is similar to those for initial and differential low field permeability and RMS MBN.

3.3. HACOM online measurements

The HACOM device is installed at a hot dip galvanising line within the processing section after the skin pass stand. Fig. 7 shows the HACOM signal over strip length for a MA steel. Changes in skin pass level are clearly seen in the $R_{p0.2}$ values calculated from HACOM amplitudes by polynomial regression. Not all HACOM amplitudes correlate well with the different process parameters like skin pass levels and temperatures. The best were found by regression algorithms in a training phase and then these can be used for calculation of interesting technological quantities like R_m and $R_{p0.2}$.

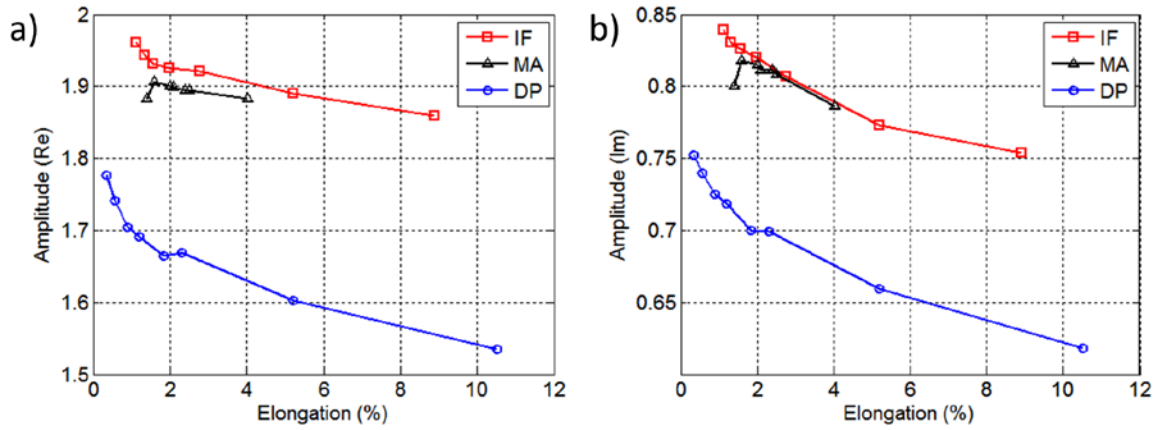


Fig. 6. Real (a) and imaginary (b) components of HACOM measurements

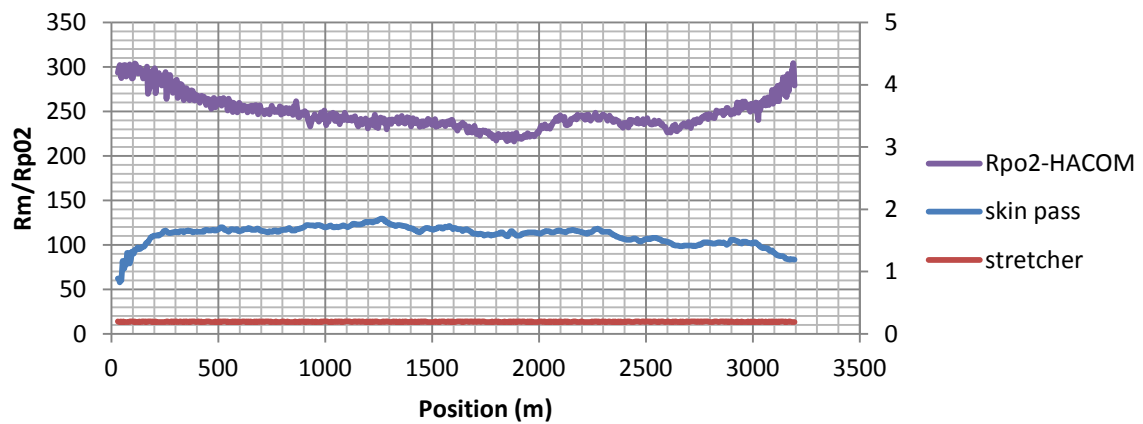


Fig. 7. HACOM signal over strip length for a MA steel

4. Online measurements from Impulse Magnetic Process Online Controller (IMPOC)

4.1. IMPOC functional principal

The measuring principle employed by the IMPOC system is based on a magnetisation and read back principle using two identical sensors, arranged on the upper and underside of the strip. Each measuring head consists of an oil cooled magnetising coil, and a magnetic field probe (Fig. 8). The running strip is magnetised periodically by the two magnetising coils up to saturation. The highly sensitive magnetic field probes measure the gradient of residual magnetic field strength in A/m² on both sides of the steel strip. The subsequent averaging of the gradient from the two measured values largely compensates for the influence of vibration on the strip. The mechanical parameters of the steel strip (i.e. tensile strength and yield strength) can then be assigned to this gradient via correlations.

Two IMPOC systems are installed on a hot dip galvanising line (HDGL) of ArcelorMittal Eisenhüttenstadt GmbH (AMEH). One system is implemented in front of and another behind the skin pass mill in the production line. The magnetic properties of the material can be influenced by a lot of variables, such as strip tension, internal stress and strip vibrations, so determination of effects caused by the skin pass process is more complex than the laboratory experiments shown in earlier sections. Another factor is the relatively low grade of skin passing in the production process shown here; values up to 1.7% in comparison to up to ~10% in experimental studies.

4.2. IMPOC test results

Fig. 9 shows in-line data for IF, MA and DP coils. The results shown here are selected to illustrate the behaviour mentioned in the previous section and are not typical process data.

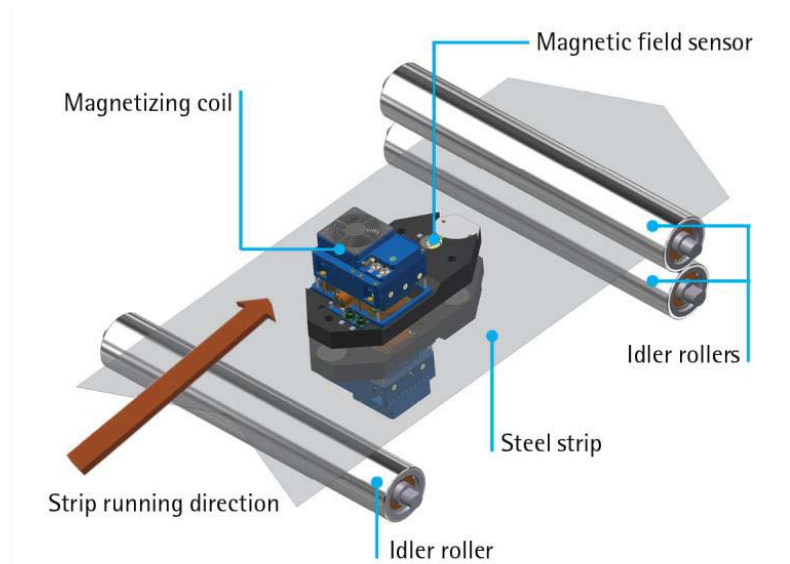


Fig. 8. Schematic diagram of IMPOC operating principle [5]

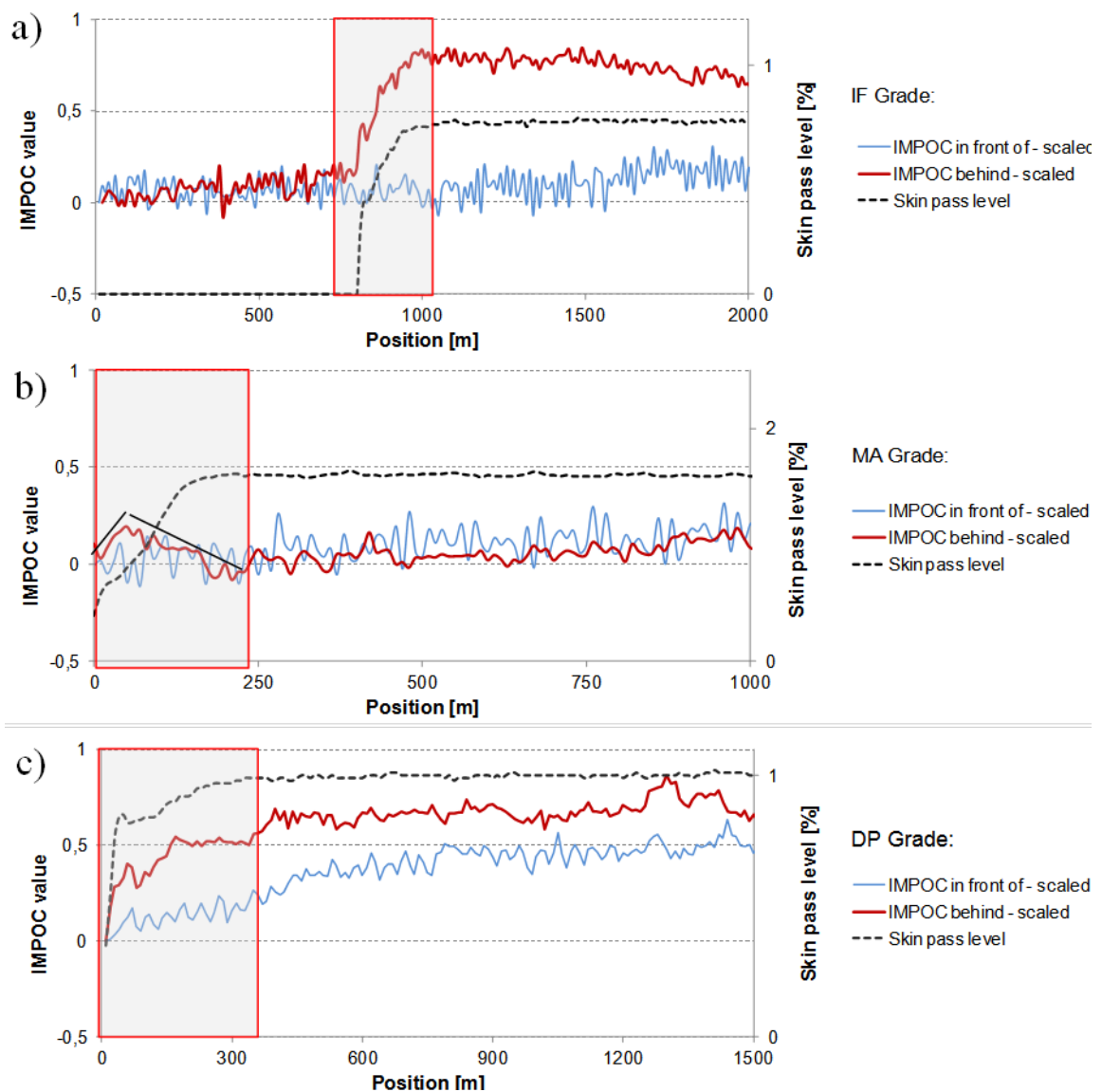


Fig. 9. IMPOC results from skin pass process for IF (a), MA (b) and DP (c) materials

The absolute IMPOC values after the skin pass process are higher for IF and MA grades compared to the values before the skin pass mill, whereas DP grades show the opposite behaviour. However, this effect is eliminated by the scaling procedure used here. Investigations concerning the different behaviour of the steel grades are currently underway.

For the IF steel (Fig. 9a) the scaled IMPOC data shows the same behaviour at both systems. When starting the skin pass process the magnetic values generated by the IMPOC system behind the mill (red line) increases noticeably. For the MA steel, the curve for the system in front of the skin pass mill (red line in Fig. 9b) shows non-linear behaviour in comparison to the skin pass level over the first 150 m. Thereafter the qualitative behaviour of the curve matches the system in front of the mill (blue line). The effect on the in-line measured data is not as clear as it is for the IF grade and the results require further investigation. For the DP grade (Fig. 9c) the skin pass level increases very fast and a clear correlation between skin pass level and IMPOC measurements does not seem to exist. Further investigation is required to establish the link between magnetic properties and skin pass level for the DP grade, including the complexity introduced by the martensitic phase.

5. Conclusions

This paper has reviewed research towards the understanding and application of the relationship between the magnetic properties of different steels and the skin pass level. Initially, the links between the magnetic properties (coercive field, MBN, permeability) and the percentage elongation of skin passed samples was reported for three different steels (IF, MA and DP). The results show that coercive field increases consistently with increasing percentage elongation for all three steels. Conversely, an inverse trend was observed for differential maximum permeability and similar results were reported for MBN and initial / differential low field permeability measurements for IF and DP steel, but the behaviour for the MA samples appears to be more complex.

Finally, the paper considered the response of two on-line measurement systems that exploit these magnetic relations, showing that skin pass level had a significant effect on both systems although here the DP steel showed an inconsistent relationship between magnetic measurement and skin pass level, albeit at low skin pass levels.

Acknowledgement

The research leading to these results has received funding from the European Union's Research Fund for Coal and Steel (RFCS) research programme under grant agreement nr. RFSR-CT-2013-00031.

References

- [1] J W Wilson, N Karimian and A J Peyton, Electromagnetic measurements for the assessment of skin passed steel samples, The 54th Annual Conference of The British Institute of Non-Destructive Testing, Telford, UK, September 2015.
- [2] M Soto, A Martínez-de-Guerenu, K Gurruchaga and F Arizti, A completely configurable digital system for simultaneous measurements of hysteresis loops and Barkhausen noise, IEEE Transactions on Instrumentation and Measurements, vol. 58, no. 5, pp. 1746–1755, 2009.
- [3] J W Wilson, N Karimian, J Liu, W Yin, C L Davis, and A J Peyton, Measurement of the magnetic properties of P9 and T22 steel taken from service in power station, Journal of Magnetism and Magnetic Materials, vol. 360, pp. 52-58, 2014.
- [4] B Heutling, W Reimche, A Krys, L Grube, M Stock, Fr.-W Bach, J Kroos, M Stolzenberg and G Westkämper, Online NDE of mechanical-technological material characteristics of steel strips via Harmonic Analysis of Eddy Current Signals, The 11th ISEM, Versailles, France, May 2003.
- [5] EMG Automation GmbH, Germany, "IMPOC_Spec_2014_Rev01_EN.pdf": 6